TEMPERATURE DISTRIBUTION IN FLOWING FILMS

E. G. Vorontsov and O. M. Yakhno

UDC 532.54

The analogy between momentum transport in a turbulent flow and heat transfer is used to discuss the temperature distribution in a flowing film; the film flowing under gravitation is considered as consisting of three zones: a laminar sublayer of thickness δ_0 with a linear velocity distribution, a transition zone, and a turbulent one.

The temperature distribution incorporates the effects from the energy dissipation in the laminar sublayer ($0 \leq y \leq \delta_0$), and this can be derived from the equation

$$w_x \frac{\partial t}{\partial x} = a \frac{\partial^2 t}{\partial y^2} + \frac{\mu}{c_p \rho g} \left(\frac{dw_x}{dy} \right)^2 . \tag{1}$$

The boundary conditions in that case take the form

$$t(y, x) = t_0 \quad \text{for} \quad x = 0, \quad \text{(initial section)}$$
$$t(y, x) = \varphi_1(x) \quad \text{for} \quad y = 0, \quad \text{(at wall)}$$
$$t(y, x) = \varphi_2(x) \quad \text{for} \quad y = \delta_0, \quad \text{(at boundary is laminar}$$

It is assumed that there is no temperature discontinuity at the tube wall, in which case the following solution to (1) is obtained:

$$\Delta t = t_{wa} - t_0 = \frac{\omega_0^2 \mu}{2\lambda} \left[\exp\left(-\frac{20}{\mathrm{Pe}} \cdot \frac{x}{\delta_0} \right) - 1 \right] . \tag{2}$$

If we assume that the temperature of the liquid is t_0 at $y = \delta_0$, while it is $t = t_s$ at $y = \delta_0 + \delta_s$, with $t = t_{gas}$ at the surface of the film ($y = \delta$), then we can [1] put as follows:

for the transitional region

$$t_t - t_0 = \frac{q_s}{\rho g c_p} \int_{\delta_0}^{(\delta_0 + \delta_n)} \frac{dy}{a + \varepsilon} , \tag{3}$$

where the upper limit to the integral is $(\delta_0 + \delta_t) < \delta_{re}$;

for the turbulent layer

$$t_{gas} - t_t = \frac{q_g}{\rho g c_p} \int_{(\delta_0 + \delta_t)}^{\delta} \frac{dy}{\varepsilon} . \tag{4}$$

From (2)-(4) we get the overall temperature difference:

$$t_{gas} - t_0 = \frac{q_t}{\rho g c_p} \int_{\delta_0}^{(\delta_0 + \delta_t)} \frac{dy}{a + \varepsilon} + \frac{q_T}{\rho g c_p} \int_{(\delta_0 + \delta_t)}^{\delta} \frac{dy}{\varepsilon} . \tag{5}$$

*All-Union Institute of Scientific and Technical Information.

Translated from Inzhenerno-Fizicheskii Zhurnal, Vol. 28, No. 4, pp. 735-757, April, 1975.

This expression incorporates the temperature difference in the transitional zone (first term) and in the turbulent region; this enables one to refine the previous method of calculation [2] and to determine Δt analytically for the transition region if the value of δ is known, which in the general case is

$$\varepsilon = \frac{\tau_{\text{п}}}{\rho g} \cdot \frac{dy}{dw} - \nu. \tag{6}$$

NOTATION

$a = \lambda / c_p \rho$	is the molecular heat-transport coefficient;
c_p	is the specific heat of the liquid at the average temperature;
ρ	is the liquid density;
g	is the acceleration due to gravity;
t	is the local temperature;
w_x	is the longitudinal velocity component;
x and y	are the coordinates;
t_0	is the liquid temperature at the boundary of the laminar sublayer;
t_t	is the temperature of the liquid at the boundary between the transitional and turbulent zones;
t_{wa}	is the temperature of the wall;
δ_0, δ_t, and δ	are the thicknesses of the laminar sublayer, transitional region, and film as a whole, respectively;
Pe	is the Péclet number;
ν	is the kinematic viscosity;
μ	is the dynamic viscosity.

LITERATURE CITED

1. S. Goldstein (editor), Modern Developments in Fluid Dynamics, Vol. 2, Dover (1938).
2. A. E. Dukler, Chem. Eng. Progr., 55, No. 10, 62-67 (1959); Symp. Ser., No. 30, 1-10 (1960).

Dep. 2765-74, April 16, 1974.
Original article submitted April 26, 1973.

FRACTIONAL-STEP METHOD IN NUMERICAL CALCULATION OF NONSTATIONARY PARAMETER DISTRIBUTIONS IN HETEROGENEOUS CHEMICAL PLANT

V. V. Yusifov

UDC 536.24.02

The fractional-step method has been used in numerical calculation of nonstationary parameter distributions (component concentrations and temperatures in a reaction mixture and at the surface of a catalyst, flux speed and density, pressure in a layer), as well as processes involving variable physical factors (heat- and mass-transfer factors, diffusion, thermal conduction, viscosity, layer resistance and specific heat), together with kinetic quantities (velocity, heat of reaction, and reaction-rate constants), all of which are described by the following systems of equations:

$$\frac{\partial}{\partial\theta}(M_Y Y) = K_Y (S - Y) + H; \quad m\frac{\partial}{\partial\theta}(MU) = (L + K)U + K_U V; \tag{1), (2}$$

$$\frac{\partial\rho}{\partial\theta} = -k_8 \operatorname{div} G; \quad \operatorname{div} P = k_7 G v; \quad G = \rho v \quad (0 \leq r \leqslant 1, \quad 0 < x \leqslant 1, \quad 0 \leqslant \theta \leqslant \theta_h) \tag{3), (4}$$

subject to the following boundary conditions:

a) at $r = 0$ $\quad \dfrac{\partial U}{\partial r} = \dfrac{\partial \rho}{\partial r} = 0;$

b) at $\theta = 0$ $\quad U_r = U_{rH};$

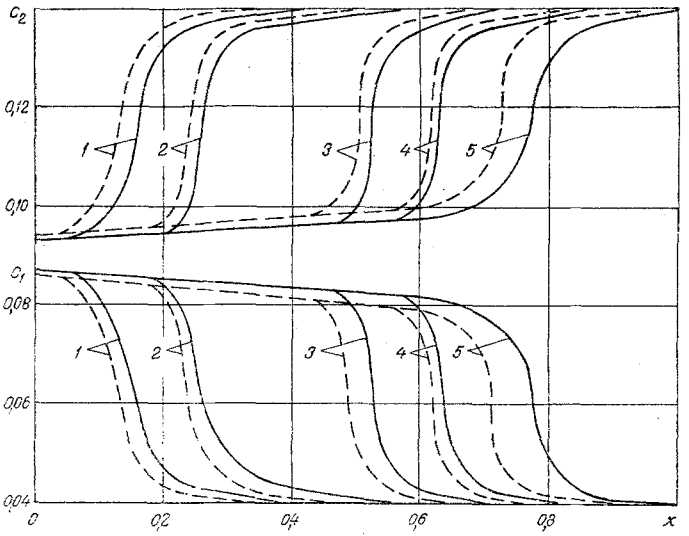

Fig. 1. Distributions of concentrations for CO (c_1), CO_2 (c_2), for the first layer of catalyst; 1) t = 3 min; 2) 6; 3) 12; 4) 14; 5) 17 min; solid line for the gas, broken line for the catalyst surface.

$$\begin{aligned}
&\text{c) at } r = l \quad \lambda_r \operatorname{grad}_r T = T_r, \quad \frac{\partial C}{\partial r} = \frac{\partial \rho}{\partial r} = 0;\\
&\text{d) at } x = 0 \quad A_x \operatorname{grad}_x U = U_x, \quad \rho = \rho_0, \quad G = G_0;\\
&\text{e) at } x = l \quad \frac{\partial U}{\partial x} = \frac{\partial \rho}{\partial x} = \frac{\partial G}{\partial x} = 0.
\end{aligned} \tag{5}$$

The operator L is replaced by the difference operator Λ; the resulting equation is separated, and (2) is solved by the predictor-corrector method to give the following difference equations:

$$\begin{aligned}
&(\alpha m^{n+\frac{1}{2}} + \beta m^n)\,[(MU)^{n+\frac{1}{2}} - (MU)^n] = \tau\,[\Lambda_1(\alpha U^{n+\frac{1}{2}} + \beta U^n) + (\alpha F^{n+\frac{1}{2}} + \beta F^n)];\\
&(\alpha m^{n+1} + \beta m^{n+\frac{1}{2}})\,[(MU)^{n+1} - (MU)^{n+\frac{1}{2}}] = \tau\,[\Lambda_2(\alpha U^{n+1} + \beta U^{n+\frac{1}{2}})];\\
&(M_Y Y)^{n+\frac{1}{2}} = \left(M_Y^n - \frac{\tau}{2} K_Y^n\right) Y^n + \frac{\tau}{2}\,[(K_Y S)^n + H^n];\\
&(M_Y Y)^{n+1} = (M_Y Y)^n + \tau K_Y^{n+\frac{1}{2}} (S^{n+\frac{1}{2}} - Y^{n+\frac{1}{2}}) + \tau H^{n+\frac{1}{2}}.
\end{aligned} \tag{6}$$

The system (6) is solved via special algorithms.

The Crank–Nicholson scheme is first applied to (3); the finite-difference scheme using fractional steps is then applied to the equation, using (3) with $\theta = 0$, and also (4) and additions d) and e) of system 5, which define ρ and G with the corresponding subscripts.

An example is given of a calculation of an industrial process for carbon monoxide conversion; some results are given in Fig. 1.

NOTATION

z and l	are the coordinates;
t	is the time;
C_m (m = 1,..., s), X_m	are the concentrations of component m in the flow and at the surface of the catalyst;
T_y and T_z	are the flow temperature at the surface of the catalyst and temperature of the cooling agent;
ϑ	is the linear flow speed;
ρ, ρ_1	are the densities of flow and catalyst bed;
P	is the pressure in layer;
D_{rm} and D_{xm}	are the effective diffusion coefficients for component m (r and m, radial and longitudinal directions);

λ_r, λ_x, η_r, η_x are the effective thermal conductivity and viscosity;
c_v and c_v^c are the specific heats of reaction mixture and catalyst;
α_{vm} is the mass-transfer coefficient for component m;
k_v and k_r are the heat-transfer coefficients for the flow–catalyst and bed–wall cases or vice versa;
λ_{c1} and ε are the bed resistance factor and porosity;
E is the unit matrix;
R_k and Q_k are the reaction rate and heat of reaction;
M_m is the molecular weight of component m;
$\nu_{m,k}$ is the stoichiometric factor for component m in reaction k;
τ is the increment in θ;
Λ_1, Λ_2 are the finite-difference operators to approximate L_1 and L_2, respectively:

$$L = L_1 + L_2; \quad L_1 = \frac{1}{r}\operatorname{div}(H_r \operatorname{grad}_r); \quad L_2 = a\operatorname{div}(A_x \operatorname{grad}_x) + b\operatorname{div}(B_x);$$

$$\alpha + \beta = 1; \quad F = KU + K_U V;$$

$$U = \begin{bmatrix} C \\ T \\ v \end{bmatrix}; \quad Y = \begin{bmatrix} X \\ y \end{bmatrix}; \quad V = \begin{bmatrix} X \\ y \\ 0 \end{bmatrix}; \quad m = \begin{bmatrix} m_1 \\ m_1 \\ m_2\rho \end{bmatrix}; \quad M = \begin{bmatrix} \rho \\ c_v\rho \\ E \end{bmatrix}; A_x = \begin{bmatrix} \rho D_x \\ \lambda_x \\ \eta_x \end{bmatrix};$$

$$A_r = \begin{bmatrix} \rho D_r \\ \lambda_r \\ \eta_r \end{bmatrix}; \quad B_x = \begin{bmatrix} G \\ c_v G \\ E \end{bmatrix}; \quad a = \begin{bmatrix} a_1 \\ a_1 \\ a_1 \end{bmatrix}; \quad b = -b_1 \begin{bmatrix} 1 \\ 1 \\ G \end{bmatrix};$$

$$K = -\frac{1}{\varepsilon}\begin{bmatrix} k_1 \\ k_2 \\ k_3 \end{bmatrix}; \quad K_U = \frac{1}{\varepsilon}\begin{bmatrix} k_1 \\ k_2 \\ 0 \end{bmatrix}; \quad A_G = G\begin{bmatrix} 1 \\ c_v \\ 1 \end{bmatrix}; \quad M_Y = \begin{bmatrix} E \\ c_v^c \end{bmatrix}; \quad K_Y = \begin{bmatrix} k_4 \\ k_5 \end{bmatrix};$$

$$S = \begin{bmatrix} C \\ T \end{bmatrix}; \quad H = \begin{bmatrix} W \\ Q \end{bmatrix}; \quad W = k_0 R; \quad R = (R_1, \ldots, R_s); \quad Q = k_0 Q_\alpha;$$

$$C = (c_1, \ldots, c_s); \quad X = (x_1, \ldots, x_s); \quad D_r = (D_{r1}, \ldots, D_{rs}); \quad D_x = (D_{x1}, \ldots, D_{xs});$$

$$R_m = \rho_1 M_m \left[\sum_{k=1}^{\alpha} \nu_{m,k}(\mp R_k)\right]; \quad Q_\alpha = \rho_1 \left[\sum_{k=1}^{\alpha} (\pm Q_k) R_k\right];$$

$$\alpha_v = (\alpha_{v1}, \ldots, \alpha_{vs}); \quad H_r = rA_r; \quad T_r = k_r(T - T_z)z_0; \quad U_x = l_0(A_G U - A_{GH} U_H);$$

$$m_1 = \frac{\varepsilon z_0^2}{t_0}; \quad m_2 = z_0^2 k_v; \quad a_1 = \left(\frac{z_0}{l_0}\right)^2; \quad b_1 = \frac{z_0^2}{\varepsilon l_0}; \quad k_1 = z_0^2 \alpha_v; \quad k_2 = \frac{z_0^2}{\varepsilon l_0};$$

$$k_3 = z_0^2 \lambda_c k_c; \quad k_4 = k_0 \alpha_v; \quad k_5 = k_0 k_v; \quad k_6 = \frac{t_0}{l_0}; \quad k_7 = l_0 k_c \lambda_{c1}; \quad \lambda_c = \lambda_{c1} G;$$

$$k_0 = \frac{t_0}{(1-\varepsilon)\rho_1}; \quad r = \frac{z}{z_0}; \quad x = \frac{l}{l_0}; \quad \theta = \frac{t}{t_0}.$$

Dep. 2763-74, September 7, 1974.
Original article submitted August 6, 1973.

DIRECTIONAL CRACKING OF GLASS BY A CO_2-LASER BEAM

V. G. Andreev

UDC 536.3

Experiments are reported on the effect of focussed CO_2-laser radiation on rotating glass tubes; a uniform ring crack is produced after a certain period, which breaks the tube into two parts.

The effect is explained via a theoretical discussion of the interaction of the beam with the glass below the phase-transition point. The thermal-conduction problem is solved for such a tube exposed to a CO_2 laser around a ring of finite height, with the initial and boundary conditions given in general form. Particular attention is given to a tube everywhere at the same initial temperature and with no internal cooling, and

a simple expression is derived for the temperature, with graphs illustrating the distribution as a function of time in the median plane at the internal and external surfaces. A quasistationary temperature distribution over the thickness is established within about 1 sec.

The heating produces thermoelastic and bending stresses; the temperature distribution gives expressions for the thermoelastic stresses in the median plane and the bending stresses in the axial direction. The thermoelastic stresses are found to be much larger than the bending ones. Graphs are presented for the thermoelastic stress distribution in the radial coordinate, and a comparison is made with the yield point of the material. It is found that a glass tube breaks as a ring crack, and this arises on the inner surface in response to circumferential tensile stress, and spreads to the outer wall in response to the axial tensile stresses.

Dep. 2764-74, September 23, 1974.
Original article submitted December 10, 1973.

DETERMINATION OF THE ADIABATIC INDICES OF REAL GASES AT HIGH PRESSURE

I. ADIABATIC INDICES OF AMMONIA

A. M. Rozen, Ya. S. Teplitskii,
E. A. Tsukerman, and V. A. Tapkhaev

UDC 536.711

As is known, upon an increase in pressure the properties of gases differ considerably from the properties of an ideal gas, i.e., it becomes impossible to use equations of the thermodynamics of ideal gases for calculations of processes of expansion and compression.

A method of deviation coefficients is proposed in [1] and the fundamental thermodynamic processes for real gases are analyzed on its basis. Some data are also presented on the values of the adiabatic indices for several real gases (two adiabatic indices are introduced, the temperature index $\varkappa$ and the volumetric index K_V, and the two do not coincide with respect to C_P/C_V). The present report is devoted to ammonia. The method of deviation coefficients was used for the calculations. Remember that deviation coefficients are the name for the ratios of the P–V–T derivatives of a real and an ideal gas:

$$\mu_P = \left(\frac{\partial V}{\partial T}\right)_P \Big/ \left(\frac{\partial V_{i\partial}}{\partial T}\right)_P = \frac{P}{R}\left(\frac{\partial V}{\partial T}\right)_P, \quad (1)$$

$$\mu_T = \left(\frac{\partial V}{\partial P}\right)_T \Big/ \left(\frac{\partial V_{i\partial}}{\partial P}\right)_T = -\frac{P^2}{RT}\left(\frac{\partial V}{\partial P}\right)_T, \quad (2)$$

$$\mu_V = \left(\frac{\partial P}{\partial T}\right)_V \Big/ \left(\frac{\partial P}{\partial T}\right)_{V_{i\partial}} = \frac{T}{P}\left(\frac{\partial P}{\partial T}\right)_V = \frac{\mu_P}{\mu_T}. \quad (3)$$

The coefficient of compressibility $Z = PV/RT$ is also a deviation coefficient. Using the method of deviation coefficients one can show [1] that for a real gas the adiabatic temperature index is

$$\varkappa = \frac{C_P}{C_P - AR\mu_P} = \frac{C_P}{C_{V_{i\partial}}}, \quad (4)$$

where $C_{V_{i\partial}}$ is the heat capacity of the process at a constant ideal volume; the adiabatic volumetric index is

$$K_V = \frac{C_P Z}{C_V \mu_P} = \frac{C_P}{C_V K_{TT}}, \quad (5)$$

where $K_{TT} = -P/V(\partial V/\partial P)_T$.

An adiabatic process is then described by the equations

$$T_2/T_1 = (P_2/P_1)^{\frac{\varkappa-1}{\varkappa}} \text{ and } PV^{\overline{K}_V} = \text{const}. \quad (6), (7)$$

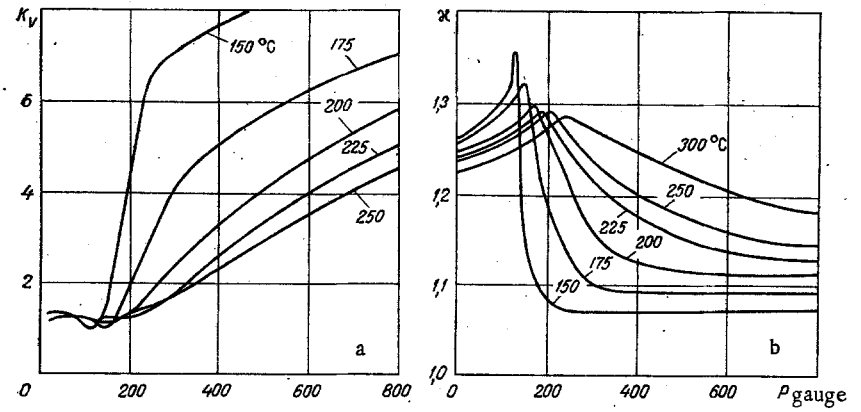

Fig. 1. Dependence of adiabatic volumetric and temperature indices K_V (a) and $\varkappa$ (b) on the pressure. P_{gauge}, kgf/cm^2.

We calculated the adiabatic volumetric and temperature indices for ammonia in the temperature range t = 150-300°C and the pressure range P_{gauge} = 0-800 kgf/cm^2 from the data of [2, 3] and Eqs. (4) and (5) and we constructed graphs of K_V and $\varkappa$ as functions of the pressure (Fig. 1a and b). As seen from Fig. 1a with an increase in pressure K_V increases sharply. This is connected with the fact that at high pressures a gas approaches a liquid in properties (for a liquid $K_V \approx 10^4$). The values of the adiabatic indices obtained were used in calculations of the characteristics of ammonia jet devices operating with supercritical parameters. Good convergence of the theoretical characteristics with the experimental data was obtained in this case.

LITERATURE CITED

1. A. M. Rozen, Zh. Prikl. Khim., No. 9 (1945); Zh. Fiz. Khim., No. 9 (1945); Dokl. Akad. Nauk SSSR, 20, No. 3 (1950);
2. Ya. S. Kazarnovskii and M. Kh. Karapet'yants, Zh. Fiz. Khim., 17, No. 3 (1943).
3. F. Din, Thermodynamic Functions of Gases, Vol. 1, London (1956).

Dep. 2905-74, October 22, 1974.
Original article submitted December 27, 1973.

CALCULATION OF TWO-DIMENSIONAL FLOW IN A NOZZLE OF A GAS CONTAINING PARTICLES

N. V. Pashatskii

UDC 532.529.5

The case of the two-dimensional flow of an incompressible gas containing solid particles is examined in the report. It is assumed that the projections of the velocities u and u_s of the gas and the particles on the nozzle axis, the gas pressure p, and the density ρ_s of the solid phase depend only on the coordinate x.

Neglecting the force effect of the particles on the gas in the direction of the y axis and expressing the projections u and v of the gas velocity through the stream function Ψ, we can write the equation of motion of the gaseous phase for the y axis [1] in the following form:

$$\frac{\partial \Psi}{\partial y} \cdot \frac{\partial^2 \Psi}{\partial x^2} = \frac{\partial \Psi}{\partial x} \cdot \frac{\partial^2 \Psi}{\partial x \partial y}. \quad (1)$$

Equation (1) is solved with the following boundary conditions. The nozzle axis (the x axis) is simultaneously a streamline. The curve L(x) of the nozzle profile is also a streamline.

The volumetric flow rate of the gas through the initial cross section of the nozzle (x = 0) is constant and equal to V.

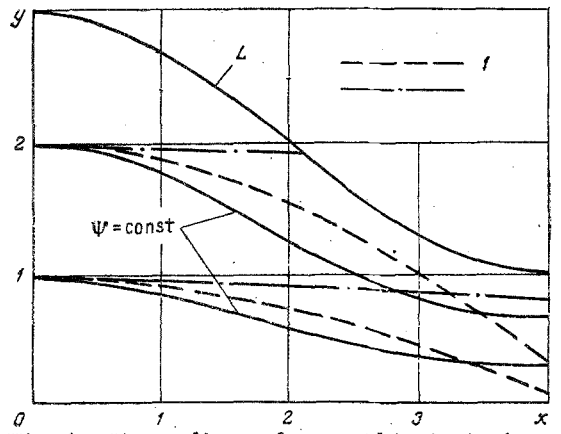

Fig. 1. Streamlines of gas and trajectories of motion of solid particles: 1) particles 2 μ in diameter; dot-dashed line – 10 μ.

Setting $\Psi(x, y) = XY$, where X is a function only of x and Y is a function only of y, we find the general solution of Eq. (1):

$$\Psi(x, y) = (Ay + B)\exp Cx.$$

The particular solution with allowance for the boundary conditions has the form

$$\Psi = V\frac{y}{L}. \qquad (2)$$

The expression (2) satisfies Eq. (1) if the nozzle profile L(x) is described by the equation $L = a\exp(-bx)$, where a and b are constants.

Calculations showed that Eq. (1) with the substitution of (2) is satisfied with sufficient accuracy for nozzles with different variable radii of curvature.

The projections of the velocities u_s and v_s of the solid particles and the trajectories of their motion are found by a method developed in [2].

As an example, we will examine in the report the motion of an air–solid particle mixture (diameter of particles 2 and 10 μ) in a flat nozzle with a profile $L = \cos(\pi/4)x + 2$.

Initial data: size of exit cross section of nozzle 2.5 mm, velocities of gas and particles at entrance equal 25 m/sec, density of particle material 3600 kg/m^3.

The results of the calculation of the streamlines of the gas and the trajectories of the particles are shown in Fig. 1. The particles 10 μ in diameter are entrained by the gas considerably less strongly than the particles 2 μ in diameter.

LITERATURE CITED

1. L. P. Vereshchaka, N. S. Galyun, A. N. Kraiko, and L. E. Sternin, Izv. Akad. Nauk SSSR, Mekh. Zhidk. Gaza, No. 3, 123-128 (1968).
2. D. T. Karpukhovich and K. F. Ivanov, Inzh.-Fiz. Zh., 22, 173 (1972).

Dep. 2907-74, October 25, 1974.
Original article submitted January 23, 1974.

PLASMA ACCELERATOR WITH AN APPLIED MAGNETIC FIELD OF AN INDUCTIVE STORAGE

V. M. Gurov

UDC 538.323.533.9

The basic characteristics of the acceleration process in the case of the application of the magnetic field of an inductive energy storage (IES) to the discharge chamber of the accelerator are analyzed in the report on the assumption that the IES magnetic field is concentrated in the volume of the storage, is uniform over the discharge chamber, and the intensity vector of this field is perpendicular to the velocity vector of the plasma.

The basic equations describing the plasma acceleration and the transitional processes in the accelerator circuit, on the assumption of an exponential law of variation of the current during the IES discharge, have the following dimensionless form:

$$\frac{d^2y_1}{d\tau^2} = qy_3^2 + 2q\gamma y_3[\exp(-\tau) + y_3], \qquad (1)$$

$$\frac{dy_3}{d\tau} = \frac{1}{1+y_1}\left[(r-\gamma y_2)\exp(-\tau) - y_3(p+\gamma y_2) - y_3 y_2\right]. \quad (2)$$

The system of Eqs. (1), (2) was solved numerically with variation of the parameters entering into it and with the initial conditions $y_1 = y_2 = y_3 = 0$ at $\tau = 0$.

It was established through a study of the equations that an increase in the fraction of inductive acceleration leads to intensification of the process of energy transfer from the storage to the kinetic energy of the cluster, although the maximum velocities attained by the plasma in the course of time are the same.

The decrease in the level of the discharge current with an increase in the contribution of the inductive acceleration in comparison with accelerators without an applied magnetic field, which leads to a decrease in the erosion of the electrodes, is important.

It is established that a change to a superconducting IES does not lead to a significant increase in the efficiency of the acceleration process, which speaks in favor of dissipative storage devices.

NOTATION

y_1, y_2, y_3 and τ	are the dimensionless path travelled by the accelerating plasma, its dimensionless velocity, the dimensionless discharge current, and the dimensionless time, respectively;
q	is the energetic parameter;
r, p	are the dimensionless parameters of discharge circuit [1];
γ	is the parameter characterizing the effect of the inductive coupling on the process of electrodynamic acceleration of the plasma.

LITERATURE CITED

1. V. M. Gurov and N. A. Khizhnyak, Zh. Tekh. Fiz., 38, 37 (1968).

Dep. 2902-74, July 8, 1974.
Original article submitted July 25, 1974.

STABILITY OF FLOW OF A LIQUID LAYER OVER THE SURFACE OF A VERTICAL CYLINDER

N. V. Zavarzin and V. M. Suyazov

UDC 532.135

In connection with the wide application of film modes of flow in many technological processes of the chemical industry and thermal-power engineering it is interesting to study their hydrodynamic stability.

The stability of flow of a layer of liquid of Grad's model, which describes suspensions of low concentration, over the surface of a vertical cylinder in a gravitational field is analyzed in the article. The solution is by the method of successive approximations, where the wave number of the disturbances (small longwave disturbances of the toroidal type were analyzed) was used as the minor parameter. It is shown that with an increase in the thickness of the descending film the flow over the inner and outer surfaces of a cylinder becomes unstable. For a given mode of flow there exists a certain characteristic Reynolds number Re^0 such that for $Re < Re^0$ the flow over the inner surface of the cylinder is more unstable than that over the outer surface. For $Re > Re^0$ the opposite picture is observed.

It is established that both flows become stable with an increase in the surface tension, whereas allowance for the rotation of particles of the suspension leads to destabilization of streams over a cylinder.

The axial asymmetry of the stress tensor for a Grad liquid does not affect the velocity of propagation of waves over the surface of a descending layer. Just as for a Newtonian liquid the velocity of wave propagation over the outer surface of the cylinder is greater than over the inner surface.

Dep. 2908-74, September 12, 1974.
Original article submitted March 16, 1973.

DEVELOPMENT OF GRADIENT FLOW OF A CONTINUOUS MEDIUM WITH A RHEOLOGICAL POWER LAW AND A CRITICAL SHEAR STRESS IN A ROUND TUBE

L. A. Luneva, A. M. Makarov, and V. G. Sal'nikov

UDC 532.54;532.135

The direct and inverse problems of the development from a state of rest of the one-dimensional flow of a continuous medium with a Herschel–Bulkley rheological equation in a cylindrical tube of constant diameter under the effect of a pressure gradient which varies with time are analyzed below in a continuation of [1].

A continuous medium of density ρ with a rheological equation in the form

$$\tau = \left(\tau_0 \left|\frac{\partial u}{\partial x}\right|^{-1} + k_n \left|\frac{\partial u}{\partial x}\right|^{n-1}\right) \frac{\partial u}{\partial x} \quad \text{for } |\tau| > \tau_0 \tag{1}$$

(τ is the tangential shear stress, τ_0 is the critical tangential shear stress, u is the velocity of the medium, and k_n is the rheological constant) fills a cylindrical tube of radius a ($0 \leq x \leq a$) and at the time t = 0 is set into motion from a state of rest under the effect of a pressure gradient P(t) which varies with time.

In the case under consideration the equation has the form

$$\rho \frac{\partial u}{\partial t} = \frac{1}{x} \cdot \frac{\partial}{\partial x} (\tau x) - P(t). \tag{2}$$

Simple operations lead to the problem describing the flow of a continuous medium in the plastic zone in dimensionless variables:

$$\frac{\partial}{\partial x}\left(\frac{1}{x} \cdot \frac{\partial (T+S)\, x}{\partial x}\right) = \frac{\partial}{\partial t} (T^{1/n}), \tag{3}$$

$$T(x, t)|_{x=\Delta(t)} = 0, \tag{4}$$

$$\frac{1}{x} \cdot \frac{\partial (T+S)\, x}{\partial x}\bigg|_{x=\Delta(t)} = \frac{2S}{\Delta(t)}, \tag{5}$$

$$\frac{1}{x} \cdot \frac{\partial (T+S)\, x}{\partial x}\bigg|_{x=1} = \varphi(t), \tag{6}$$

$$\Delta(t)|_{t=0} = 1. \tag{7}$$

For the "direct problem" the function $\varphi(t)$ is assumed to be known while T(x, t) and $\Delta(t)$ are unknown; for the "inverse problem" the function $\Delta(t)$ is assumed to be known while T(x, t) and $\varphi(t)$ are unknown. $\Delta(t)$ is the boundary of separation of the zones of viscous flow and of a quasisolid core.

By integration of Eq. (3) over the spatial coordinate using the rheological law and the corresponding boundary conditions one obtains a system of integro-differential equations whose solution is constructed by the method of successive approximations.

LITERATURE CITED

1. A. M. Makarov and V. G. Sal'nikov, Inzh.-Fiz. Zh., 24, No. 6, 1088 (1973).

Dep. 2903-74, November 11, 1974.
Original article submitted June 20, 1973.

VISCOSITY OF DIBUTYLPHTHALATE AT HIGH PRESSURES AND DIFFERENT TEMPERATURES

N. A. Agaev and A. D. Yusibova

UDC 532.13:547.37.043

The esters of phthalic acid, whose thermophysical properties have not been studied, find extensive application as plasticizers and as the working fluids of hydraulic machines and mechanisms. Only data on the viscosity and density at atmospheric pressure are presented in [1], and in a limited temperature range at that.

The results of an experimental study of the viscosity of dibutylphthalate performed in the temperature interval of 20-350°C and at a pressure of from 1 to 700 kgf/cm^2 are presented in the article.

The viscosity was measured by the capillary method. A diagram of the experimental apparatus, the construction of the viscosimeter, the method of conducting the experiments, and the calculation of the viscosity are described in detail in [2-3].

Two viscosimeters were used in the experiments: the first in the temperature interval of 20-100°C and the second in the interval of 100-350°C. The matchup at the 100° isotherm showed agreement within the limits of 0.2%.

The absolute temperature for the experiments was measured by a standard platinum resistance thermometer with an accuracy of 0.02°C, and a constant experimental temperature was maintained within limits of ±0.005°C.

The pressure was created and measured with a load-piston MP-600 manometer of class 0.05.

The outflow time was measured automatically by an electrical timer with an accuracy of 0.1 sec. The measurements were made with respect to isotherms; 15 isotherms were taken.

The measurements were made twice at each point, with the reproducibility of the experiments not exceeding ±0.2 %.

The step of the pressure variation on the isotherms was 50-100 kgf/cm^2. The maximum pressure on the isotherms was 700 kgf/cm^2. The purity of the dimethylphthalate studied is characterized by the grade cp.

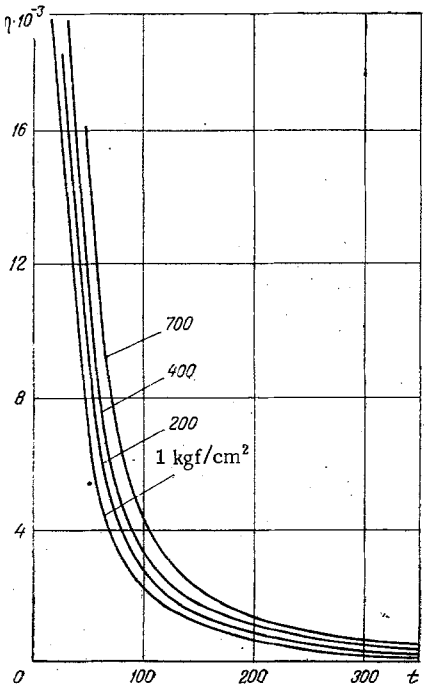

Fig. 1. Viscosity of dibutylphthalate (N·sec/m^2) at constant pressures as a function of temperature (°C).

TABLE 1. Viscosity $\eta \cdot 10^{-3}$ N·sec/m^2 of Dibutylphthalate

P, kgf/cm^2	t, °C														
	20,10	25,20	30,00	35,00	40,00	50,00	75,00	100,00	125,00	150,00	175,00	200,30	249,96	300,14	350,00
1	2026,0	1639,0	1354,0	1097,0	935,8	682,8	354,2	217,5	152,5	113,2	86,55	67,03	45,04	26,57	6,720
50	2213,0	1774,0	1468,0	1180,0	1013,0	726,7	377,0	229,5	162,0	120,5	92,00	71,38	47,78	28,29	7,510
100	2415,0	1920,0	1585,0	1273,0	1095,0	774,0	400,9	242,6	172,1	128,0	98,29	75,66	50,41	30,07	8,530
150	2621,0	2067,0	1708,0	1366,0	1177,0	820,5	424,2	256,8	181,8	135,2	103,6	79,49	53,50	32,03	9,250
200	2841,0	2234,0	1839,0	1467,0	1265,0	875,6	449,8	271,0	192,4	142,6	109,7	83,83	56,47	33,76	10,42
300	3330,0	2588,0	2134,0	1686,0	1446,0	995,7	499,7	299,5	212,5	158,4	121,2	92,30	62,49	37,34	12,23
400	3884,0	3007,0	2467,0	1935,0	1641,0	1130,0	553,5	330,0	224,7	175,2	132,7	100,3	68,34	40,88	14,10
500	4525,0	3467,0	2830,0	2213,0	1856,0	1279,0	613,4	364,7	252,7	189,6	144,3	109,2	74,12	44,20	15,57
600	5305,0	3940,0	3216,0	2505,0	2092,0	1442,0	680,1	403,3	273,2	204,5	155,5	118,0	79,95	47,53	17,12
700	—	—	—	—	—	1613,0	746,5	445,0	292,5	219,3	166,6	126,4	85,66	51,04	19,29

The experimental error of estimated to be a value on the order of ±1.0-1.5 %.

Smoothed values of the viscosity are presented in Table 1 and illustrated in Fig. 1.

The data obtained agree well, within the limits of 1-2 %, with the literature data [1].

LITERATURE CITED

1. A. J. Barlow, J. Lamb, and A. J. Matheson, Proc. Roy. Soc. A, 292, 322-342 (1966).
2. I. F. Golubev, Viscosity of Gases and Gas Mixtures [in Russian], Fizmatgiz, (1959).
3. I. F. Golubev and N. A. Agaev, Viscosity of Saturated Hydrocarbons [in Russian], Azerneshr., Baku (1964).

Dep. 2900-74, August 27, 1974.
Original article submitted October 31, 1972.

CALCULATION OF THE PROCESS OF DUST COLLECTION IN CLOTH FILTERS

V. A. Uspenskii, G. L. Sitnitskii, and R. G. Adamov

UDC 621.928.94/96

A mathematical description of the process of dust collection in a cloth filter is proposed in the article. The nonsteady nature of the process of filtration of a dust–gas mixture, caused by the variation in the porosity of the filter and in its thickness due to the accumulation on the filter baffle plate of a deposit of filtered dust particles, is taken into account in the description.

The deposit of dust takes place both within pores of the cloth and on its surface. The presence of intracloth and above-cloth dust layers, forming a so-called self-filter, leads to a high efficiency of dust collection.

It is assumed that during the regeneration of the filter, accomplished through an increase in its aerodynamic resistance to a certain value, only the above-cloth dust layer is completely removed. The removal of dust from within the cloth is hindered because of the high sinuosity of its pores.

The dust retention is determined by two oppositely acting factors: the deposit of dust particles on the porous baffle and their blowing off due to the aerodynamic action of the gas stream. The dust balance in the elementary above-cloth dust layer with allowance for the mechanism of dust retention leads to a system of nonlinear differential equations containing partial derivatives:

$$\begin{cases} -W\dfrac{\partial C}{\partial y} = \dfrac{\partial (mC)}{\partial t} + \dfrac{\partial \rho}{\partial t}; \\ \dfrac{\partial \rho}{\partial t} = a\left[WC(1-m) - b\rho_p W^2 \dfrac{1-m}{m^2}\right]. \end{cases} \quad (1)$$

The direction of the coordinate axis y in this case coincides with the direction of the filtration velocity W, while the point of origin for the measurement of y lies at the boundary between the cloth and the above-cloth dust layer.

There is a system of equations similar to (1) for the intracloth dust layer, with m being replaced by mm_c and b by bg. By the introduction of a certain average effective porosity m_1 each of these systems is reduced to one linear first-order differential equation of the form

$$W\frac{\partial C}{\partial y} = -m_1\frac{\partial C}{\partial t} - aW(1-m_1)\left(C - \frac{b\rho_p W}{m_1^2}\right). \quad (2)$$

The solution of (2) is found by the method of characteristics, where the additional condition for the first case is the condition of constancy of the dust concentration in the gas ahead of the filter, while in the

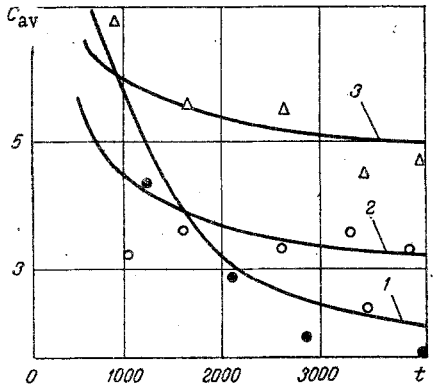

Fig. 1. Dependence of average residual dust concentration $C_{av} \cdot 10^6$, kg/m^3 on filtering time (sec) for different filtration rates [W = 0.01 m/sec (1), 0.03 (2), and 0.05 m/sec (3)] with an initial concentration $C_0 = 3 \cdot 10^{-3}$ kg/m^3 for S120 metallic cloth. Points: experiment for the corresponding curves.

second case the additional condition is the solution of (2) at y = 0. The final expression for the average over the interregeneration time period of the dust concentration C_{av} in the gas behind the filter has the form

$$C_{av} = \frac{b\rho_p W}{m_1^2}\left\{\frac{g}{m_c^2} + \left(1 - \frac{g}{m_c^2}\right)\exp\left[-a(1-m_1)\delta\right]\right\}$$
$$+ \frac{m_1^2\rho_p\left(C_p - \frac{b\rho_p W}{m_1^2}\right)}{aC_0 W t_p}\exp\left[-a(1-m_1)\delta + a\frac{C_0 m_p c}{\rho_q m_1}\right]\left[1-\exp\left(-\frac{aC_0 W t_p}{m_1^2\rho_p}\right)\right].$$

The functions obtained are confirmed experimentally (Fig. 1).

NOTATION

C	is the dust concentration in gas, kg/m^3;
m, m_c	are the porosities of dust layer and of cloth, respectively;
t	is the filtering time, sec;
ρ, ρ_p	are the density of dust deposit and of material of dust particles, respectively, kgf/m^3;
g	is the coefficient of adhesion of dust to filtering material;
a, b	are the proportionality factors, 1/m, sec/m;
C_0	is the dust concentration in gas ahead of filter, kg/m^3;
t_r	is the length of interregeneration period, sec;
δ	is the thickness of dust layer within cloth, m.

Dep. 2898-74, September 12, 1974.
Original article submitted March 25, 1974.

AN APPROXIMATE MEANS OF SOLVING HYDRO-AEROMECHANICS PROBLEMS BY THE ELECTROHYDRODYNAMIC ANALOGY (EHDA) METHOD

V. P. Tolmachev

UDC 533.6.011+532.546.013.3

Electromodeling is presently obtaining ever wider distribution as a method of solving problems from different fields of engineering. One of the important trends in the development of electromodeling is the expansion of the class of problems solvable on a specific electromodeling device.

In the present report we shall consider a means of electromodeling of hydro-aeromechanics problems by the EHDA method using the representation of the unknown functions in the form of harmonics, which allows one to use the technique of electromodeling of the Laplace equation.

We represent the continuity equation for an established axisymmetric stream of liquid (gas) in a natural orthogonal coordinate system consisting of the distance s along the streamlines and the distance η along the normal to them:

$$\frac{\partial\theta}{\partial\eta}=\frac{\partial \ln \rho wy}{\partial s}, \quad (1)$$

where θ is the angle between the stream lines and the axis of symmetry; w is the total stream velocity; ρ is the density; y is the Cartesian coordinate perpendicular to the axis of symmetry. Since Eq. (1) corresponds in the form of notation to one of the Cauchy–Riemann conditions for the functions θ and $\ln \rho wy$ we assume that the second Cauchy–Riemann condition is also satisfied:

$$\frac{\partial \ln \rho wy}{\partial\eta}=-\frac{\partial\theta}{\partial s}. \quad (2)$$

Consequently, the functions θ and $\ln \rho wy$ satisfy the Laplace equation and the electromodeling technique can be used with respect to them. The solution of the Laplace equation for θ allows one to find the geometry of the streamlines of the flow and the configuration of the boundaries (free surfaces, shock waves, etc.), while with the help of the solution of the Laplace equation for $\ln \rho wy$ we can find the distribution of the dynamic characteristics in the region studied.

To take into account the physical properties of a specific stream one uses a correction to the distribution function $\ln \rho wy$, determined by the difference between Eq. (2) and the equation of the momentum in the projection on the normal to the streamline, which are separated relative to the derivative $\partial p/\partial\eta$, where p is the pressure.

Dep. 2897-74, September 12, 1974.
Original article submitted January 23, 1974.

EFFECT OF THE MOLECULAR WEIGHT ON THE STRUCTURE AND THERMOPHYSICAL PROPERTIES OF POLYETHYLENE

V. P. Dushchenko, V. N. Smola,
E. V. Grishchenko, I. M. Kucheruk,
V. M. Baranovskii, and N. E. Menyailov

UDC 678.742:536+539.1

Polymers usually consist of a mixture of macromolecules of different sizes which is characterized by the average molecular weight (MW). Such a heterogeneity essentially determines many properties of polymers, particularly the thermophysical properties.

The purpose of the work is a study of the effect of the MW on the variation of such parameters of the crystalline structure as the degree of crystallinity $\varkappa$, the sizes L of the crystallites, and the thermophysical properties (specific heat capacity C_p, thermal conductivity coefficient λ) of low-pressure polyethylene (LPPE) with an MW of from 10,000 to 106,000.

A calorimetric study showed that in the vitreous state the passage below the glass-transition temperature (T_g), caused by the hindered motion of sections of the macromolecule chain containing four successive CH_2 groups about the collinear bonds, is observed at 153°K for all MW. In the temperature interval of devitrification both an increase in T_g (which almost ceases at MW = 100,000) and an increase in the jump ΔC_p in the specific heat capacity occur with an increase in the MW. The specific heat capacity C_p decreases with an increase in the MW. Calculations based on the hole theory by B. Wunderlich's method [1] for amorphous polyethylene lead to values of ΔC_p on the order of 11.3 J/mole · °K, whereas for our specimens the experimental values lie in the range of 0.6-1.1 J/mole · °K. Thus, it becomes clear that a considerable amount of the amorphous phase of LPPE exists in a "bound" state (through sections, sites of bends in the macromolecules between crystallites). The increases in the density of the amorphous phase of LPPE (Table 1) with an increase in the MW is a confirmation of this. The latter fact, despite the decrease in χ with an increase in MW (Table 1), leads to a decrease in the values of C_p. The specific heat capacity of LPPE with different MW at T = 300°K was also obtained through calculation using V. V. Tarasov's theory of heat capacity [2]. Good correspondence is observed between the calculated and experimental values of C_p.

TABLE 1. Degree of Crystallinity $\varkappa$, Transverse (L_{110}) and Longitudinal (L_{002}) Dimensions of Crystallites, Density ρa of Amorphous Phase, Specific Heat Capacity C_p, and Coefficient λ as Functions of the MW

MW · 10^3	10000	24500	42000	52000	62000	76000	99000	106000
$\varkappa$, %	62,5	68,6	73,4	72,5	72,5	64,7	47,0	50,0
L_{110}, Å	85,0	97,4	252,0	90,0	82,5	64,7	53,9	46,7
L_{002}, Å	43,9	82,5	142,5	172,4	190,0	198,0	201,0	212,4
ρ_a, kg/m^3	803	805	806	808	809	811	814	816
C_p, $\frac{J}{kg \cdot °K}$	1990	1843	1795	1730	1719	1690	1665	1654
λ, W/m · °K	0,5	0,49	0,46	0,46	0,45	0,43	0,39	0,39

The variations in $\varkappa$ and in the dimensions of the crystallites determine the value of λ for the specimens studied. Actually, since a crystal has smaller phonon-scattering centers than an amorphous polymer, the value of λ will decrease with a decrease in the degree of crystallinity and the dimensions of the crystallites. Consequently, the decrease in λ with an increase in the MW as a result of the decrease in $\varkappa$ and in the crystallite dimension L_{110} which is observed in these studies is weakened due to the increase in L_{002} and in the density of the amorphous phase of LPPE.

LITERATURE CITED

1. B. Wunderlich and H. Baur, Heat Capacities of Linear High-Polymers, Springer-Verlag (1972).
2. V. V. Tarasov, New Problems in the Physics of Glass [in Russian], Gostroiizdat, Moscow (1959).

Dep. 2896-74, October 2, 1974.
Original article submitted May 25, 1974.

SOME PHYSICAL PROPERTIES OF FIBROUS TUNGSTEN

D. M. Karpinos, V. S. Klimenko, Yu. V. Kondrat'ev, G. A. Duzhanskii, A. E. Rutkovskii, I. K. Senchenkov, and L. L. Sukhikh

UDC 536.21:537.311.33:621.763:669.277

Gas-permeable fibrous tungsten is a heat-resisting material suitable for use in various novel techniques, especially at very high temperatures with transpiration cooling.

Results are given on some thermophysical and mechanical properties, and also the permeability of porous (25% porosity) tungsten with an oriented fibrous structure made from tungsten fibers of diameter 25-30 μm.

The strength of this 25% porosity tungsten exceeds the strength of various forms of compact tungsten at all temperatures between room values and 2800°K, being only slightly inferior to the rhenium-alloyed compact and rolled tungsten.

The thermal conductivity and resistivity were determined by Kohlrausch's static method between room temperature and 1300°K at pressures below 10^{-4} mm Hg; the coefficient of variation for the thermal conductivity was 5-7%, and for the resistivity, 1.2-1.8 %.

TABLE 1

°K	473	673	873	1073	1273	1473
TEC · 10^6, deg^{-1}	3,86	4,05	4,24	4,35	4,38	4,42

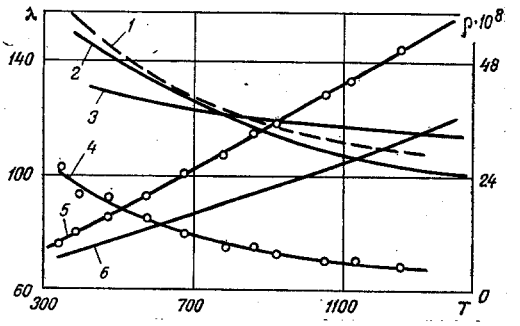

Fig. 1. Thermal conductivity and electrical conductivity as functions of temperature: 1) thermal conductivity of fibrous tungsten converted to the pore-free state; 2 and 3) thermal conductivity of compact tungsten (handbook); 4 and 5) thermal conductivity and electrical resistance of fibrous tungsten (measured value); 6) resistance of compact tungsten (λ in W/m·deg, ρ in Ω·m, and T in °K).

Figure 1 shows the thermal conductivity and resistivity of fibrous tungsten as functions of temperature; it also shows data from reference works for compact deformed tungsten.

The conductivity characteristics of fibrous tungsten are poorer than those of the compact material on account of the reduced effective cross section, as well as contact resistance. On the other hand, there is satisfactory agreement between the thermal conductivity as calculated back to the pore-free state and the results for compact tungsten, which shows that the second factor is unimportant, i.e., there is good contact between the fibers in the material. is satisfactory agreement between the thermal conductivity as calculated back to the pore-free state and the results for compact tungsten, which shows that the second factor is unimportant, i.e., there is good contact between the fibers in the material.

The thermal-expansion coefficient (TEC) was measured as a function of temperature with a Chevenart quartz dilatometer for the range 300-1500°K in argon; the coefficient of variation did not exceed 1.5%. The temperature dependence of the coefficient increases monotonically in this range. Table 1 gives the mean values averaged over five specimens.

The permeability was measured from the flow rate of gas through a flat specimen at pressure differences up to 30 atm, and it indicated that the flow was nearly laminar, the permeability coefficient being $0.5\text{-}1.5 \cdot 10^{-9}$ cm^2 for porosities of 10-35%.

Dep. 2909-74, September 12, 1974.
Original article submitted July 28, 1969.

THERMAL CONDUCTIVITY OF POTASSIUM CARBONATE

V. Ya. Chekhovskii and G. I. Stavrovskii

UDC 536.2

The thermal conductivity of potassium carbonate K_2CO_3 has been measured at 250-700°C; a static method was used with a radial heat flux in argon at 1.2 atm, this gas filling the sealed equipment after removal of the air. The specimens were weighed from the white anhydrous crystalline powder of chemically pure grade as follows: the powder of particle size less than 0.5 mm was dried in a desiccator at 160°C for 1 h and then pressed in a mold at 1 t/cm^2. Potassium carbonate loses its absorbed water and water of crystallization above 152°C, and gives the anhydrous salt. This is hygroscopic, so the prepared specimens are stored in a desiccator and removed directly before insertion in the apparatus. The density after the experiment was 1.600 g/cm^3, which goes with the density of pore-free potassium carbonate, 2.418 g/cm^3, to define the true porosity as 34 %.

The results may be approximated via the following formula with the temperature in °K:

$$\lambda = (0{,}326 + 0{,}00479\ T)^{-1}\ \text{W} \cdot \text{m}^{-1} \cdot \text{deg}^{-1}$$

The 0.95 confidence range in relative terms for results from this formula is 5-10%; similarly, the confidence range at the 0.95 level for the systematic error is ± 6 .

The following are recommended values of the thermal conductivity calculated from this formula:

T, °K	500	600	700	800	900	1000
λ, $\frac{\text{W}}{\text{m} \cdot \text{deg}}$	0.367	0.312	0.271	0.240	0.215	0.195

Dep. 2901-74, May 6, 1974.
Original article submitted July 5, 1973.

ESTIMATION OF THE ERROR DUE TO THE TWO-DIMENSIONAL TEMPERATURE DISTRIBUTION IN THE MEASUREMENT OF THE THERMAL CONDUCTIVITY OF A FILM

V. A. Arutyunov, L. Ya. Lyubin, and M. N. Pivovarov

UDC 536.21

The temperature distribution in an orthotropic disk is discussed; the initial equation is

$$\lambda_z \frac{\partial^2 T}{\partial z^2} + \lambda_r \frac{1}{r} \cdot \frac{\partial}{\partial r}\left(r \frac{\partial T}{\partial r}\right) = 0. \tag{1}$$

The boundary conditions ($h = \alpha_r/\lambda_r$) are

$$T = T_1 \text{ at } z = 0,\ T = T_2 \text{ at } z = \delta,\ \partial T/\partial r = h(T_1 - T) \text{ at } r = r_0. \tag{2}$$

If the recording instrument registers the heat flux through a circular spot of radius r_1 at $z = \delta$, we have ($r_1 \leq r_0$; $R_0 = r_0/\delta$; $R_1 = r_1/\delta$) that

$$\frac{\lambda_{zr}}{\lambda_z} = \frac{4h\delta}{R_0 R_1}\left(\frac{\lambda_r}{\lambda_z}\right)^{3/2} \sum_{n=1}^{\infty} \frac{\operatorname{cth} \mu_n}{\mu_n^2 + (h\delta)^2 \lambda_r/\lambda_z} \cdot \frac{J_1(\mu_n \sqrt{\lambda_z/\lambda_r}\, R_1)}{J_0(\mu_n \sqrt{\lambda_z/\lambda_r}\, R_0)}, \tag{3}$$

$$\mu_n J_1(\mu_n \sqrt{\lambda_z/\lambda_r}\, R_0) = h\delta \sqrt{\lambda_r/\lambda_z}\, J_0(\mu_n \sqrt{\lambda_z/\lambda_r}\, R_0).$$

The narrow-band asymptotic method can be used for $\sqrt{\lambda_z/\lambda_r} r_0 \gg 1$ to obtain a more convenient expression for estimating the error; (1) becomes

$$\Lambda^2 \frac{\partial^2 T}{\partial \varsigma^2} = -\frac{\varepsilon^2}{\rho} \cdot \frac{\partial}{\partial \rho}\left(\rho \frac{\partial T}{\partial \rho}\right), \quad \Lambda^2 = \frac{\lambda_z}{\lambda_r}, \quad \rho = \frac{r}{r_0}, \quad \varsigma = \frac{z}{\delta}. \tag{4}$$

As $\varepsilon = \delta/r_0 \ll 1$, the problem is a singularly perturbed one; to solve it one needs not only the external asymptotic expansion [the solution to (4): $T = T^{(0)} + \varepsilon T^{(1)} + \ldots$] but also the internal one $t = t^{(0)} + \varepsilon t^{(1)} + \ldots$, which is a solution to the equation

$$\Lambda^2 \frac{\partial^2 t}{\partial \varsigma^2} + \frac{\partial^2 t}{\partial \eta^2} + \varepsilon(1 + \varepsilon\eta + \ldots)\frac{\partial t}{\partial \eta} = 0, \quad \eta = (r_0 - r)/\delta. \tag{5}$$

These expansions must satisfy the conditions

$$T = T_1 \text{ at } \varsigma = 0,\ T = T_2 \text{ at } \varsigma = 1,$$
$$\partial t/\partial \eta = h(t - T_1) \text{ at } \eta = 0,\ (T^{(0)} + \varepsilon T^{(1)} + \ldots)_{r \to r_0} \sim (t^{(0)} + \varepsilon t^{(1)} + \ldots)_{\eta \to \infty}.$$

The first terms in the expansions ($T^{(0)}$, $t^{(0)}$) are used to estimate the error of measurement for the transverse thermal conductivity with the recorder placed above and below; for $\zeta = 1$ we have

$$\frac{\Delta\lambda_z}{\lambda_z} = \frac{4\alpha_r \delta^2}{\pi^2 r_0 \lambda_z} \sum_{n=1}^{\infty} \frac{\exp(-n\pi \sqrt{\lambda_z/\lambda_r}\, \eta_1)}{n(n + \alpha_r \delta/\pi \sqrt{\lambda_r \pi_z})}; \quad \Delta\lambda_z = \lambda_{zr} - \lambda_z, \quad \eta_1 = (r_0 - r_1)/\delta.$$

If $r_1 = r_0$ and $\alpha_r \delta \ll \pi\sqrt{\lambda_r \lambda_z}$ we have

$$\frac{\Delta\lambda_z}{\lambda_z} = \frac{2\alpha_л \delta^2}{3 r_0 \lambda_z} \quad \varsigma = 1, \quad \frac{\Delta\lambda_z}{\lambda_z} = -\frac{1}{3} \cdot \frac{\alpha_л \delta^2}{\lambda_z r_0} \quad \varsigma = 0.$$

If $r_0 - r_1 \ll \delta\sqrt{\lambda_r/\lambda_z}$, then $\Delta\lambda_z \ll 4\alpha_r \delta^2/(\pi^2 r_0)$; for instance, for $(r_0 - r_1)\delta = 0.22 \times \sqrt{\lambda_r/\lambda_z}$ we have $\Delta_z \approx 0.236\, \alpha_r \delta^2/r_0$.

NOTATION

T	is the temperature;
δ and r_0	are the thickness and radius of disk;
λ_z and λ_r	are the transverse and longitudinal thermal conductivities;
λ_{zr}	are the recorded transverse thermal conductivity;
α_r	is the effective radiative-transfer factor.

Dep. 2904-74, November 12, 1974.
Original article submitted December 30, 1973.

THERMAL STRESS BUILDUP IN SOLID-STATE LASER ELEMENTS

G. I. Zheltov and G. G. Meshkov

UDC 621.378.32

A solid-state laser working in the continuous-wave regime for high-frequency pulsed state responds to any change in the mean pumping power with temperature changes in the rod, and hence in the internal thermal stresses, which influence the optical parameters of the material and hence the stability of the spatial and other characteristics of the output.

The thermal-stress buildup has been calculated for a cylindrical rod; the quasistatic theory of thermoelasticity is applied in the homogeneous approximation for heat release in the rod. The results are presented as tables and graphs, which allow one to perform engineering estimates of the thermal stresses as functions of time.

Measurements have also been made on the thermal-stress buildup in glass and ruby rods; the thermal stresses were determined from the induced optical anisotropy.

The measurements are compared with calculations, and it is found that the error in the calculations does not exceed 15% at heating levels more than 0.5 of the maximum.

Dep. 2895-74, September 20, 1974.
Original article submitted May 29, 1974.

CALCULATION OF ADIABATIC PROCESSES FOR $N_2O_4 \rightleftharpoons 2NO_2 \rightleftharpoons 2NO + O_2$ GAS MIXTURES

G. M. Novik and B. I. Lomashev

UDC 534.174

A method is given for calculating nonequilibrium flows of a dissociating mixture of gases in channels of variable cross section; it uses the adiabatic parameters with the usual assumptions of gasdynamics.

The method is as follows:

1. An integral form is given for the adiabatic equations, and this is used with Bernoulli's equation for the flow and the equation of continuity to get

$$\left[\frac{C_n S_n}{S_{n+2}\left(\frac{T_n}{T_{n+1}}\right)\frac{1}{K_v-1}}\right]^2 = \frac{2gK_p}{K_p-1} P_n V_n \left[1-\left(\frac{T_{n+1}}{T_n}\right)^{\frac{K_T}{K_p}\cdot\frac{K_p-1}{K_T-1}}\right]. \quad (1)$$

Conditions are imposed in the steps in the longitudinal coordinate, which gives the temperatures T_{n+1} at section n + 1 in the channel.

2. From T_{n+1} the value of the pressure P_{n+1} is found from the adiabatic equation.

3. The component concentrations at section n + 1 are found from equations obtained by direct integration of the differential equations for the reaction kinetics.

4. The known values for T_{n+1}, P_{n+1}, and the component concentrations are used with the appropriate equations to find the volume V_{n+1} and gas feed C_{n+1}.

5. The nonequilibrium adiabatic parameters required to calculate the flow at the next step are found from equations derived from the internal-energy equation, the adiabatic equation, and the equation of state for the gases:

$$K_v = 1 + \frac{1+\alpha_1+\alpha_1\alpha_2}{f_1} + \frac{f_2 V}{f_1 T}\left(\frac{\Delta\alpha_1}{\Delta V}\right) + \frac{f_3 V}{f_1 T}\left(\frac{\Delta\alpha_2}{\Delta V}\right), \quad (2)$$

$$K_T = 1 - \frac{f_2 + (1+\alpha_2)T}{f_1 + 1 + \alpha_1 + \alpha_1\alpha_2} \cdot \frac{P}{T} \cdot \frac{\Delta\alpha_1}{\Delta P} -$$

$$- \frac{f_3 + \alpha_1 T}{f_1 + 1 + \alpha_1 + \alpha_1\alpha_2} \cdot \frac{P}{T} \cdot \frac{\Delta\alpha_2}{\Delta P} - \frac{1 + \alpha_1 + \alpha_1\alpha_2}{f_1 + 1 + \alpha_1 + \alpha_1\alpha_2}, \quad (3)$$

$$K_p = K_T \frac{K_v - 1}{K_T - 1}, \quad (4)$$

where α_1 and α_2 are the degrees of dissociation in the first and second stages of the reaction, with f_1, f_2, and f_3 the composition function and the characteristic vibrational frequencies of the components.

The method has been used in an algorithm for calculating gas-mixture flows in such channels with a Minsk-22 computer; the run time is short for Mach numbers of 1; and the results are of high accuracy, so it is assumed that this scheme can be used in design calculations for particular gas mixtures and systems.

Dep. 2906-74, September 25, 1974.
Original article submitted March 28, 1974.

SIMULATION OF NONSTATIONARY THERMAL CONDUCTION WITH NONLINEAR OUTPUT FROM INTERNAL SOURCES

A. V. Archakov and L. I. Gutenmakher

UDC 536.24.02

When the nonlinear equation for nonstationary thermal conduction is handled with network models, it is necessary to supply the nonlinear current $I_w(U_m)$ to the nodes, where U_m is the potential at node m, and w is the subscript indicating that this simulates the nonlinear power output from internal sources.

To avoid laborious iterative methods of specifying $I_w(U_m)$ it is suggested that one should simulate a nonlinear drain by means of a current generator with a controlled internal resistance R_i; when certain conditions are met, the corresponding current is given by

$$I_w = V/R_i, \quad (1)$$

where V is the potential external to the RC network, which considerably exceeds the voltage at the nodal point. Then $R_i(U_m)$ can be varied in accordance with (1) by applying an arbitrary control law I_w.

This controlled resistance R_i has been realized via a circuit in which each capacitor in the network is periodically connected to resistors R_0 and R via a high-frequency electronic switch, which are such that the effective resistance is a function of time:

$$R(t) = \begin{cases} R, & (\nu-1)\theta \leqslant t < (\nu-1)\theta + \tau; \\ R_0, & (\nu-1)\theta + \tau \leqslant t < \nu\theta; \\ \nu = 1, 2, 3, \ldots, \end{cases} \quad (2)$$

where t is current time and Θ is the switching period, whose length is much less than the solution time for the RC model; $\tau \in [0, \Theta]$.

The transient response for circuits of this type indicates that in this case the equivalent controlled circuit resistance (which is also the internal resistance R_i of the current source) becomes a function of the interval τ:

$$R_i = \frac{\theta R R_0}{\theta R - \tau(R - R_0)}. \quad (3)$$

The interval τ is produced by a pulse-width modulator, which controls U_m, and then from (1) and (3) the current supplied to the node becomes a function of U_m.

The maximum error in defining the nonlinear drain $I_w(U_m)$ is given by

$$\delta_{max} = \frac{\theta(R - R_0)}{4RR_0C}, \quad (4)$$

where C is the capacitance at the node.

The error was not more than 0.5 % under the conditions of the experiment; the principle is also suitable for realizing a nonlinear thermal conductivity and nonlinear boundary conditions of types II, III, and IV.

Dep. 2899-74, April 16, 1974.
Original article submitted October 9, 1973.

VARIATIONAL DERIVATION OF THE THERMAL-DIFFUSION EQUATIONS FOR THIN PLATES AND SHELLS

R. N. Shvets and M. S. Ravrik

UDC 539.377

The variational principle has been used to write a system of differential equations for the mean temperature t and solute concentration c:

$$h^2\Delta T_1 - b_1T_1 - b_2T_2 - \frac{h^2}{a}\cdot\frac{\partial}{\partial\tau}(T_1+\gamma_c c_1) = -(b_1t_1^c + b_2t_2^c),$$

$$h^2\Delta T_2 - 3(1+b_1)T_2 - 3b_2T_1 - \frac{h^2}{a}\cdot\frac{\partial}{\partial\tau}(T_2+\gamma_c c_2) = -3(b_2t_1^c + b_1t_2^c),$$

$$h^2\Delta c_1 + h^2d_0\Delta T_1 - \varepsilon_1(d_0T_1+c_1) - \varepsilon_2(d_0T_2+c_2) - \frac{h^2}{D_c}\cdot\frac{\partial c_1}{\partial\tau} = -\frac{1}{d_c^{e,T}}(\varepsilon_1\mu_1^c + \varepsilon_2\mu_2^c),$$

$$h^2\Delta c_2 + h^2d_0\Delta T_2 - 3(1+\varepsilon_1)(d_0T_2+c_2) - 3\varepsilon_2(d_0T_1+c_1) - \frac{h^2}{D_c}\cdot\frac{\partial c_2}{\partial\tau} = -\frac{3}{d_c^{e,T}}(\varepsilon_2\mu_1^c + \varepsilon_1\mu_2^c) \quad (1)$$

and the corresponding boundary conditions at the ends:

$$\nabla^i T_1 n_i + h_t(T_1 - T_1^b) = 0, \quad \nabla^i T_2 n_i + h_t(T_2 - T_2^b) = 0,$$
$$\nabla^i(D_tT_1 + D_cc_1)n_i + H(d_T^{e,c}T_1 + d_c^{e,T}c_1 - \mu_1^b) = 0, \quad (2)$$
$$\nabla^i(D_tT_2 + D_cc_2)n_i + H(d_T^{e,c}T_2 + d_c^{e,T}c_2 - \mu_2^b) = 0,$$

which are Euler–Ostrogradsky equations for the variational problem $\delta I = 0$ on the assumption that the temperature and concentration are linearly distributed over the thickness of the shell, via which heat and mass transfer occur in accordance with Newton's law. Here

$$b_{1,2} = \frac{h}{2}(h_t^+ \pm h_t^-); \quad \varepsilon_{1,2} = \frac{h}{2}(H_1^+ \pm H_1^-); \quad H_1 = \frac{H}{L};$$

$$t_{1,2}^c = \frac{1}{2}(t_c^+ \pm t_c^-); \quad \mu_{1,2}^c = \frac{1}{2}(\mu_c^+ \pm \mu_c^-);$$

$$\gamma_c = -\frac{d_T^{e,c}}{C^{e,c}}T_0; \quad d_0 = \frac{d_T^{e,c}}{d_c^{e,T}}; \quad \Delta = \frac{1}{AB}\left[\frac{\partial}{\partial\alpha}\left(\frac{B}{A}\cdot\frac{\partial}{\partial\alpha}\right) + \frac{\partial}{\partial\beta}\left(\frac{A}{B}\cdot\frac{\partial}{\partial\beta}\right)\right];$$

with $C^{e,c}$ the specific heat at constant volume and concentration; $d_T^{e,c}$, $d_c^{e,T}$ are coefficients representing the variation in the chemical potentials of the particles in response to the concentration and temperature respectively; T_0 is absolute temperature; L is a coefficient representing the atomic mobility of the diffusing material; $h_0^{\pm}$, $tH_1^{\pm}$ are the relative heat- and mass-transfer coefficients; $t_c^{\pm}$, $\mu_c^{\pm}$ are the temperatures and chemical potentials of the diffusing material in the medium around the surfaces at $z = \pm h$; D_t and D_c are diffusion coefficients; a is the thermal diffusivity; n_i is the vector of the external normal to the shell surface; ∇^i, ∇i are symbols for the contravariant and covariant differentiation with respect to the coordinates α and β; T_1^b, T_2^b and μ_1^b, μ_2^b are the mean temperatures and chemical potentials at the ends; A and B are the coefficients in the first quadratic form for the median surface of the shell; and τ is time.

Similarly, coupled equations are derived for the mean values of T_1, T, μ_1, and μ_2, in particular when the definitive parameters are the temperature t and chemical potential μ. This system can be derived from (1) via the equations of state

$$\mu_1 = d_c^{e,T}c_1 + d_T^{e,c}T_1, \quad \mu_2 = d_c^{e,T}c_2 + d_T^{e,c}T_2. \quad (3)$$

An example handled via (1) is the solute concentration redistribution on account of uneven heating in an infinite plate with a circular hole of radius R, the material being a two-component solution of concentration c_0. Heat and mass transfer to the environment occur through the surface of the plate, the temperature and chemical potential of the environment remaining constant. Particular cases are discussed.

Dep. 2894-74, September 30, 1974.
Original article submitted June 14, 1973.

COORDINATE DEPENDENCE OF THE HEAT-TRANSFER COEFFICIENT FOR A THIN SEMI-INFINITE ROD

Yu. I. Babenko

UDC 536.24.01

The problem of heat transfer in a uniformly cooled thin semi-infinite rod initially at absolute-zero temperature is discussed:

$$\left[\frac{\partial}{\partial t} - \frac{\partial^2}{\partial x^2} + \gamma(x)\right] T = 0, \quad 0 \leqslant x < \infty, \quad 0 < t < \infty,$$

$$T|_{x=0} = T_0(t); \quad \left.\frac{\partial T}{\partial x}\right|_{x=0} = q_0(t); \quad T|_{x=\infty} = 0; \quad T|_{t=0} = 0 \tag{1}$$

(T is the temperature, x is the coordinate, t is the time, and γ is the heat-transfer function). It is required to determine $\gamma(x)$ with the use of an "excess" boundary condition. The author has previously obtained a relationship between T_0, q_0, and γ as a series in fractional-order derivatives:

$$-q_0 = D^{1/2} T_0 + \frac{\gamma(0)}{2} D^{-1/2} T_0 + \frac{\gamma'(0)}{4} D^{-1} T_0 + \frac{\gamma''(0) - \gamma^2(0)}{8} D^{-3/2} T_0 + \ldots \tag{2}$$

If T_0 and q_0 are specified in the series form

$$T_0 = \sum_{n=0}^{\infty} a_n t^{n/2}, \quad q_0 = \sum_{n=0}^{\infty} b_n t^{(n-1)/2}; \quad a_n, \; b_n - \text{const}, \tag{3}$$

then by the substitution of (3) into (2) and equating of the coefficients of like powers of t it is possible to determine successively all the derivatives $\gamma^n(0) = (\partial^n\gamma/\partial x^n)_{x=0}$ and so the function $\gamma(x)$ itself in the form of a Taylor series in powers of x.

Dep. 2893-74, August 8, 1974.
Original article submitted May 29, 1974.